Image Cover Sheet

CLASSIFICATION	SYSTEM NUMBER 514412
UNCLASSIFIED	

TITLE

Improved Landmine Detection Capability \(ILDC\): Systematic Approach to the
Detection of Buried Mines Using Passive IR Imaging

System Number:

Patron Number:

Requester:

Notes:

DSIS Use only:

Deliver to:

	Form Approved OMB No. 0704-0188

Report Documentation Page

Public reporting burden for the collection of information is estimated to average 1 hour per response, including the time for reviewing instructions, searching existing data sources, gathering and maintaining the data needed, and completing and reviewing the collection of information. Send comments regarding this burden estimate or any other aspect of this collection of information, including suggestions for reducing this burden, to Washington Headquarters Services, Directorate for Information Operations and Reports, 1215 Jefferson Davis Highway, Suite 1204, Arlington VA 22202-4302. Respondents should be aware that notwithstanding any other provision of law, no person shall be subject to a penalty for failing to comply with a collection of information if it does not display a currently valid OMB control number.

1. REPORT DATE **10 OCT 2000**	2. REPORT TYPE	3. DATES COVERED **00-00-2000 to 00-00-2000**

4. TITLE AND SUBTITLE	5a. CONTRACT NUMBER
Improved Landmine Detection Capability (ILDC): Systematic approach to the detection of buried mines using passive IR imaging	5b. GRANT NUMBER
	5c. PROGRAM ELEMENT NUMBER
6. AUTHOR(S)	5d. PROJECT NUMBER
	5e. TASK NUMBER
	5f. WORK UNIT NUMBER

7. PERFORMING ORGANIZATION NAME(S) AND ADDRESS(ES) **Defence Research and Development Canada - Suffield,P.O. box 4000 Stn Main,Medicine Hat, Alberta T1A 8K6,**	8. PERFORMING ORGANIZATION REPORT NUMBER
9. SPONSORING/MONITORING AGENCY NAME(S) AND ADDRESS(ES)	10. SPONSOR/MONITOR'S ACRONYM(S)
	11. SPONSOR/MONITOR'S REPORT NUMBER(S)

12. DISTRIBUTION/AVAILABILITY STATEMENT
Approved for public release; distribution unlimited

13. SUPPLEMENTARY NOTES

14. ABSTRACT
In order to reduce the serious problem associated with the mining of important supply f communication roads by hostile parties during peace keeping operations, the Canadian Department of National Defence has recently begun the development of a multi-sensor teleoperated mine detection vehicle, the Improved Land-Mine Detection Capability (ILDC). One sensor identified as a serious candidate for that project is a passive IR camera. In the past, many organizations have assessed the efficiency of this technique of detection and reported widely fluctuating results. It is believed that the main reason for these fluctuations is associated with the ad hoc interpretations used by different researchers. In this paper, a more systematic analysis is presented which takes into account variables such as time of the day, time of the year, weather conditions, type of road and many others. A working model is proposed in order to facilitate the prediction of theIR signature of the buried land-mines and is compared with data acquired from multiple trials. These trials were done with live mines (without fuzes) and surrogates buried in different types of road (packed gravel and sand) and during different times of the day and different times of the year.

15. SUBJECT TERMS

16. SECURITY CLASSIFICATION OF:			17. LIMITATION OF ABSTRACT	18. NUMBER OF PAGES	19a. NAME OF RESPONSIBLE PERSON
a. REPORT **unclassified**	b. ABSTRACT **unclassified**	c. THIS PAGE **unclassified**	**Same as Report (SAR)**	**14**	

Standard Form 298 (Rev. 8-98)
Prescribed by ANSI Std Z39-18

This page is left blank

This page is left blank

Improved Landmine Detection Capability (ILDC): Systematic approach to the detection of buried mines using passive IR imaging

Jean-Robert Simard

Threat Detection Group, Defence Research Establishment Suffield,
Box 4000, Medicine Hat, AB, Canada T1A 8K6

ABSTRACT

In order to reduce the serious problem associated with the mining of important supply/communication roads by hostile parties during peace keeping operations, the Canadian Department of National Defence has recently begun the development of a multi-sensor teleoperated mine detection vehicle, the Improved Land-Mine Detection Capability (ILDC). One sensor identified as a serious candidate for that project is a passive IR camera. In the past, many organizations have assessed the efficiency of this technique of detection and reported widely fluctuating results. It is believed that the main reason for these fluctuations is associated with the ad hoc interpretations used by different researchers. In this paper, a more systematic analysis is presented which takes into account variables such as time of the day, time of the year, weather conditions, type of road and many others. A working model is proposed in order to facilitate the prediction of the IR signature of the buried land-mines and is compared with data acquired from multiple trials. These trials were done with live mines (without fuzes) and surrogates buried in different types of road (packed gravel and sand) and during different times of the day and different times of the year.
(**Keywords:** buried, mine, detection, infrared, imaging, temperature, gradient, model.)

2 INTRODUCTION

In the last 15 years, with the increase of peacekeeping activities in countries decimated by civil wars and other social disorders, the interest for mine detection and clearance has become increasingly important. To support the international effort to solve this critical problem, the Canadian Department of National Defence (DND) has put together a team of experts to design and build a multi-sensor remotely operated mine detection vehicle operating primarily on roads, the Improved Land-Mine Detection Capability (ILDC). One critical sensor of this vehicle is a passive IR camera. From recent work published by many organizations (RECON/OPTICAL Inc.,[1,2] Wackenhut Advanced Technology Corp.,[3] WES,[4] ERIM,[5] LLNL[6,7]), it is well accepted that IR technology has good capabilities to detect metal-free buried mines. However, one drawback of this technique is its performance dependency on environmental conditions (time of day, time of year, weather conditions, type of road,...). In this document, the author proposes a methodology well adapted to monitor and anticipate the fluctuations in the efficiency of IR technology in detecting buried mines.

We will first describe two models (one being a simplified version of the other) which interpret quantitatively the thermal mechanisms involved in the formation of the IR signature of buried mines. Subsequently, the validity of the quantitative parameters identified by these models is tested experimentally during trials designed especially to reproduce real operating scenarios. Throughout the trials, special attention has been given to the evaluation of the limitations associated with the use of these quantitative parameters. Then, the experimental results are

discussed as functions of the proposed models and finally, the outcome of this analysis is summarized.

3   DESCRIPTIVE MODELS

Before describing the model associated with the phenomenon of IR signature build-up of buried mines, it is important to understand the two main causes behind it. The first is the surface effect; this effect is associated with the process of disturbing the soil surface over the mine and over its immediate surroundings during the burying operation. The action of moving the soil at the surface will leave a thin layer of small rocks and sand which has poor thermal contact with the deeper soil layers. Because of the direct exposure of this thin insulated soil layer to the atmospheric radiation (mainly sun and cloud radiation), the temperature difference between the perturbed soil surface and its immediate surroundings can reach many degrees and is easily observable with an IR imager under sunny skies. It has been observed that these surface effects are detectable for many days (3 weeks in some conditions). The second phenomenon behind the build-up of the IR signature of buried mines is the volume effect. This effect is related to the presence of the buried mine and the perturbed soil layer covering it and is mainly responsible for the night-time IR signature of buried mines, the IR signature of mines buried on uncompacted roads (such as sand roads), and for mines buried for a long period (more than 6 months). The proposed models aim to describe this volume effect exclusively, leaving the investigation of the surface effect for future work.

The models proposed are based on a one-dimensional analysis of two heat loads: the soil layer where the mine is buried and that where no mine is buried (see figures 1a and 1b). These two loads are coupled by the fact that each of them receives the same heat flow at the surface and reaches the same temperature at a sufficient depth. With these conditions, it is possible to represent these two heat loads as a system where parameters can be monitored to define their state and from which the temperature contrast (the temperature difference caused by the presence of a mine) can be derived. Two models are described. The first model uses a detailed approach where the two heat loads are defined as being spatially distributed and for which the heat equation is solved. Some results derived from this model are used to characterize quantitatively the state of the buried mine system. Because the model proposed herein tries to solve a practical problem, as described in the introduction, and because some parameters of the two heat load system (depth of buried mine, compactness of soil cover,...) can fluctuate seriously for different buried mine sites, a simpler model using an electrical analogy has been developed. This second model, even if empirical, has the advantage of relating statistically the temperature gradient into the soil with the expected temperature contrast of the buried mine. In addition, this second model has the advantage of being easily applied in situ. In the section 4, the validity of the prediction of the second model will be evaluated quantitatively with experimental data obtained from realistic scenarios.

3.1   Detailed approach

A complete model describing the state of a coupled heat load system associated with a buried mine can be derived by considering the system as being spatially distributed (see figure 1a) and by solving the well known one-dimensional heat equation,

$$\frac{\partial T}{\partial t} = a \frac{\partial^2 T}{\partial z^2}.$$

(1)

In this equation, T is the temperature, t is time, z is the depth, and a is the heat diffusivity defined as the ratio between the heat conductivity and the product of heat capacity and the density. To use this equation, we assume a homogeneous soil layer where the heat properties are adequately represented locally by average values. We also assume that the soil is mostly dry and heat transfer by moisture migration is negligible. With these assumptions, the heat equation can be solved by Fourier analysis for the case of homogeneous soils (one of the two heat loads to characterize) with two boundary conditions: the surface temperature $T_r(t)$ and the temperature at large depth $T_\infty(t)$, as[8]
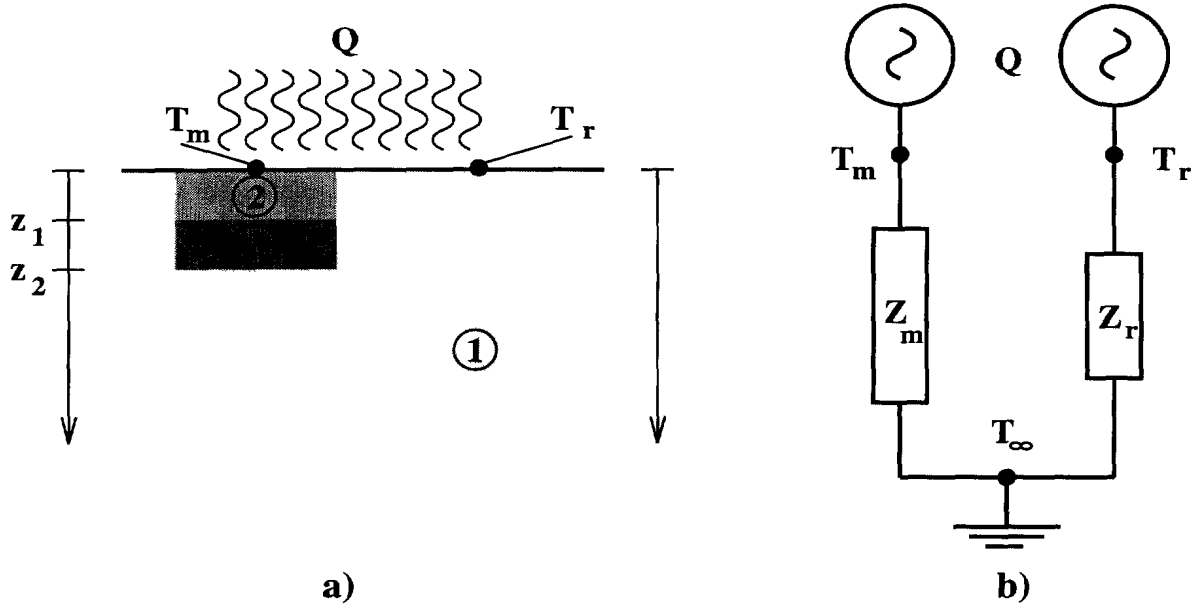
Figure 1: Schematic representations of the detailed (a) and the simple (b) models. In these two models, Q is the heat flow between the atmosphere and the soil, T_m and T_r are the apparent temperatures at the soil surface of the soil where the mine is buried and next to it (reference), T_∞ is the temperature at a sufficient depth, Z_m and Z_r are the heat impedances of the soil column containing the mine and that without the mine. The zones identified by 1,2, and 3 represent the unperturbed soil, the soil covering the buried mine and the mine, respectively.

$$T(z,t) = T_\infty(t) + \sum_{k=1}^{\infty} A_k \exp^{-z/D} \cos(k\omega t - (z/D + \phi_k)). \tag{2}$$

Furthermore, this solution could be applied separately to the three zones identified in figure 1a which represents the second heat load of the buried mine system. To solve that problem, we first need to know the parameters describing the heat properties of these three zones and then, the two following boundary conditions must be applied. continuity of the temperature and continuity of the heat flow between zones. In addition, the fact that the heat flow at the surface and the temperature at large depth have to be the same for the two heat loads defines a dependent system which is completely described by its initial state and the time evolution of the heat flow at the surface of the soil. However, as mentioned in the introduction of this section, this detailed solution can be difficult to apply for the proposed scenario because of its complexity. Moreover, the randomness associated with certain parameters defining this model (mainly the mine depth, the compactness of the soil cover, and to a certain extent, the type of the soil) reduces the applicability of this approach. In the next section, a simpler approach will be described which will provide a method to characterize the IR contrast of buried mines that is easy to apply for the proposed scenario and is more adequate to take into account the randomness of some parameters of that heat load system.

3.2 Simple approach

For this simple model, we used an electrical analogy to define the coupled system representing the two heat loads (see figure 1b). We define $\mathbf{Q}$ as the heat flow into the soil surface which is identical for all soil surfaces having similar exposure to the surroundings, $\mathbf{T_m}$ and $\mathbf{T_r}$ are the temperatures at the surface where the mine is buried and that next to it (reference), $\mathbf{Z_m}$ and $\mathbf{Z_r}$ identify the heat impedance of the soil column where the mine

is buried and reference, and $\mathbf{T_\infty}$ is the soil temperature at a sufficient depth which is identical for the two soil columns. With these definitions and the heat conduction law,

$$\Delta T = Z \times Q, \tag{3}$$

we can easily derive two empirical proportionalities describing the temperature contrast at the surface ($\mathbf{T_m} - \mathbf{T_r}$):

$$(T_m - T_r) \quad \propto \quad Q, \tag{4}$$
$$(T_m - T_r) \quad \propto \quad (Z_m - Z_r). \tag{5}$$

Even if this approach allows only limited quantitative application in the field, the equations describe adequately the inversion in contrast between night and day (the contrast will inverse as the heat flow changes direction between the soil and the atmosphere) and the direct relation between the temperature contrast and the heat impedance change created by the buried mine. However, because of the spatially distributed nature of the heat impedance of the soil column (with or without a mine), it is impractical to use directly this simple model to monitor or predict the temperature contrast of buried mines. A method to overcome this difficulty uses the conduction law (equation 3) to characterize the heat flow (Q) and to apply its linear relationship to the temperature contrast derived previously to predict the IR signature of buried mines. To do so, the temperature gradient into the ground is first evaluated by taking temperature samples at different depths. Then, the analytical solution derived above (equation 2) is fitted with these temperature samples. Subsequently, by evaluating the derivative of this analytical solution, we obtain a parameter directly proportional to the heat flow and consequently, to the temperature contrast of a buried mine. This approach is attractive by its simplicity but many questions arise. The first is the determination of the depth where the derivative is evaluated. Because the soil has to be seen as a spatially distributed heat load with capacitance and conductance properties, the heat flow will change with depth. This variation of the heat flow with depth usually expresses a phase shift between the thermal state of the soil surface and the deeper layer. An adequate approach for choosing the depth at which this derivative is evaluated is to consider the expected depth of buried mines. For the experimental results shown in the next section, it has been chosen to evaluate this derivative at 7 cm. This choice for the depth is derived from the concept that the IR signature of a buried mine is dictated by the heat flow at the depth of the buried mine (mine top face) and because we associated 7 cm to the typical maximum depth at which mechanical pressure detonated mines are buried. There are other considerations that have to be investigated with this approach: the effect of the mine depth, the spatial correlation of this temperature gradient into the soil, and the effect of the type of soil. The next section will propose some solutions.

4   EXPERIMENTAL VERIFICATION

To verify the concepts described in the previous section, different types of trials have been designed and performed in different parts of Canada. The temperature contrasts (IR signature) of the buried mines were obtained by acquiring digital images (full 12 bits) with an Agema THX-1000 LWIR camera. The temperature contrast was derived by subtracting the pixel-averaged value of a small square area at the centre of the blob created by a buried mine and the pixel-averaged value of a reference square surface close to the mine. An apparent temperature contrast was derived from these pixel values by calibrating the camera. The camera, which has a 62(h)x41(v)-degree FOV, was inclined downward by 45 degrees and placed at a height of three meters in front of a ground vehicle. The different trials reported here can be classified as two types: static trials, where small digital image acquisition of buried mine IR signatures is done at fixed time intervals with the vehicle immobile, and dynamic trials, where the digital image acquisition of buried mine IR signatures is done at fixed distance while the vehicle is moving (speeds less than 5 km/h). More details of the different trials are given below.

4.1 Characterisation of the soil temperature gradient

During each trial, one or more probes were used to sample the soil temperature at different depths. This temperature probe was built with 15 thermocouples placed at 3 cm intervals along a Plexiglas tube. After making a vertical hole with an auger into a representative area of the road, the probe was inserted and the space between the tube and the wall of the hole was filled with sand. For each trial, the 15 thermocouples were sampled at fixed time intervals (30 minutes for dynamic trials and 1 hour for static trials). Using a standard non-linear least square fit algorithm, the two first terms of the analytical solution for the temperature profile derived in the previous section (equation 2) were fitted for each discontinuous profile obtained with the probe. Examples of fits obtained are shown in figure 2a. With this analytical solution for the ground temperature profile, the derivative of the temperature with respect to depth (referred in this article as the temperature gradient) is evaluated at a depth of 7 cm. It is this specific parameter which will be used to correlate all results reported in this article.

a)   b)

Figure 2: The graph a) represents the temperature change with depth at different times of the day. The continuous lines have been obtained by joining 12 temperature readings sampled at 3 cm interval and the dashed lines are derived from the numerical fitting of the exact solution of the heat equation (equation 2) with these sampled temperatures. The graph b) shows the time evolution of the apparent contrasts of two buried mines (TMN-46 surrogates) and the measured temperature gradients over a 32-hour period in the Canadian prairies. EI and MI identify the evening and morning inversion periods respectively.

4.2 Static trials

The results of two static trials are reported in this article. The first trial was performed over a gravel packed road in the Canadian prairies during a 32-hour period beginning May 10, 1995 at 0800. For this trial, two TMN-46 anti-tank surrogates filled with a plastic having similar heat properties to TNT were buried at a depth of 5 and 7 cm respectively. These two replica mines were buried more than 8 months before the trial so that thermal surface effects were negligible. For this static trial, one digital image was taken at each hour and at the same time, and the temperature profile was sampled. Figure 2b shows the time variation of the temperature contrast of these two buried mines and the temperature gradients into the soil. We can observe on that graph the expected inversion of contrast between day and night and the inversion periods (morning and evening) where the IR signatures of the buried mines disappear. We can also observe a good correlation between the temperature

contrast and the temperature gradient [1]. To obtain a better evaluation of this correlation, figure 3a and 3b show directly the correspondence between the contrast and the gradient. We observe a good correlation between these two parameters; also, the linear coefficients derived from a first order least square fit of these points decrease with the depth of the mine as expected.
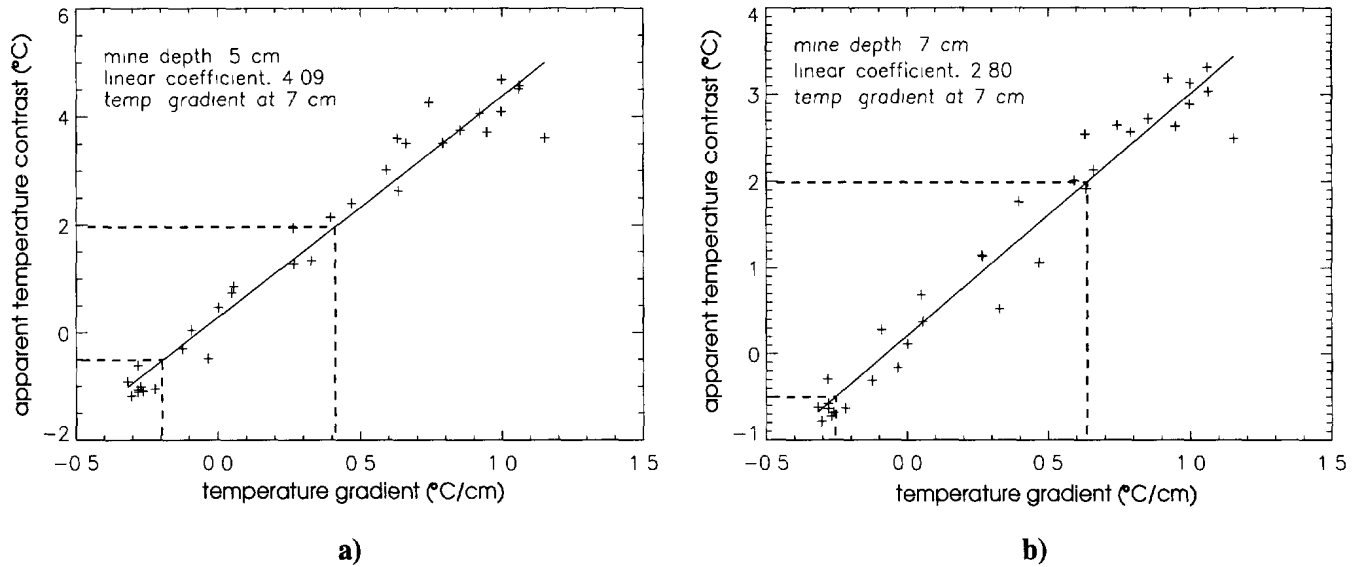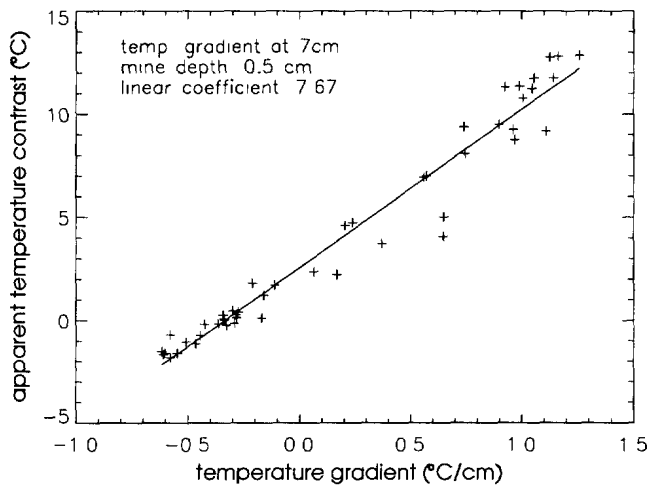

a)   b)

Figure 3: These two plots are derived from figure 2b. The + symbols show the apparent temperature contrasts corresponding to the temperature gradients. The straight lines are obtained from a standard first order polynomial fits through these points.

The second static trial, performed over a packed gravel road in the Canadian shield region during a 48-hour period beginning June 6, 1995 at 1700, was performed to evaluate the correlation between the temperature contrast and the temperature gradient in a different geological region. In this trial, three replica mines made with the same plastic as that from the previous trial, but designed to simulate the thermal mass of the Yugoslavian mine TMA-3, were buried a few days before the measurements. They were buried at depths of 0.5, 2, and 4 cm. The IR signature of a refilled hole containing no mine was also monitored for comparison. Figures 4a, 4b, 4c, and 4d show the correlation existing between the temperature gradient and the IR signature associated with these four sites. Even if the correlation shows more fluctuations when compared with the graphs obtained during the first static trial, an acceptable linear relation can still be derived. It is believed that these fluctuations are related to the presence of strong surface effects caused by recent burying. This possibility is supported by the fact that the strong fluctuations are present mainly during day-time (positive contrast) where surface effects occurred. Another important aspect is the comparable linear coefficient obtained for the mine buried at a depth of 5 cm during this trial with the one buried at a depth of 4 cm during the trial performed in the Canadian prairies (3.61 and 4.09 respectively). However, it is important to take into account the imprecision associated with the process of burying a mine at a specific depth [2] and the different heat loads of the mines used for these two trials before comparing quantitatively these linear coefficients.

---

[1]For aesthetic reasons, the temperature gradient has been multiplied by -1 to give a positive correlation with the temperature contrast of buried mines.
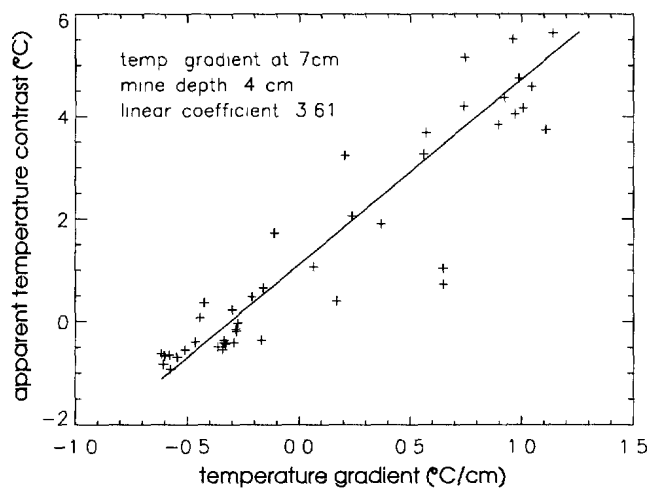
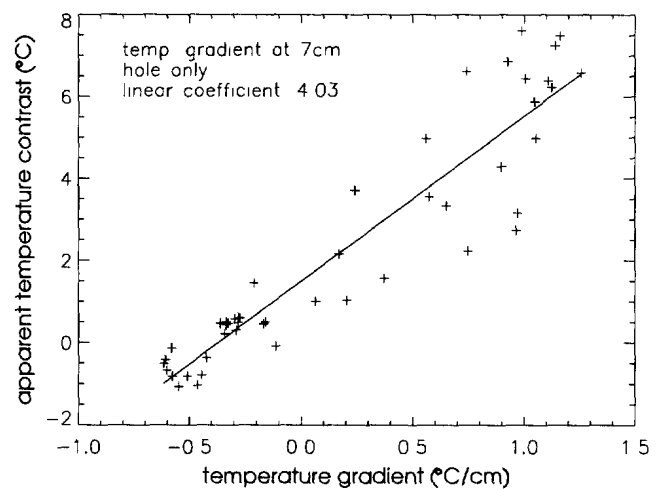[2]An imprecision of ±0.5 cm in the evaluation of the soil cover is an acceptable value for for these trials.

Figure 4: These four graphs are obtained in a similar manner than those shown in figure 3 but are plotted with the data of the trial performed in the Canadian shield. In this trial, the surrogates used were designed to reproduce the thermal characteristics of the TMA-3 mine. The large standard deviations observed during day-time (positive contrast) are associated with thermal surface effects.

4.3 Dynamic trial

The dynamic trial was designed to reproduce scenarios of interest where the IR technology might be used in peacekeeping demining operations. Two sections of road (a sand road and a packed gravel road) approximately 5 km long were chosen in the Canadian prairies. The trial was performed during the third week of July 1995 and multiple passes were performed at different times of the day and night. The same IR camera, same vehicle, and the same configuration as described previously were used. The vehicle was moving at a speed of ~3 km/h and operators, who had no idea about the number and the position of the mines placed along the road, were monitoring the IR images of the road to identify potential sites of buried mines. An observer, placed behind the operator, was receiving confirmations of the presence of mined sites in the FOV of the IR camera by communicating with the driver; this allowed him to record successful detections pointed by the operator. In addition to the analog recording of the trial, one IR digital image of the road was taken for each meter travelled over the first 3.5 km of road. Later, these digital images were used to evaluate the temperature contrast of the buried mines detected by the operator. In this trial, a mixture of different types of real anti-tank mines (TMA-3, Mk-7, M21, VS-2.2), real anti-personnel mines (VS-50, PMA-3) and surrogates were also used. Throughout that week, a temperature probe, similar to that described previously, recorded automatically the temperature profile in the ground every half hour. Figures 5a, 5b, 5c, 5d show the detection efficiency of the operator, the thermal effect (surface or volume) by which the buried mine was detected, the temperature contrast of the detected buried mines and the temperature gradient derived from the method described previously. Four different passes were performed. The passes chosen represent the four main heat states that the soil-atmosphere system passes through during a 24-hour cycle.
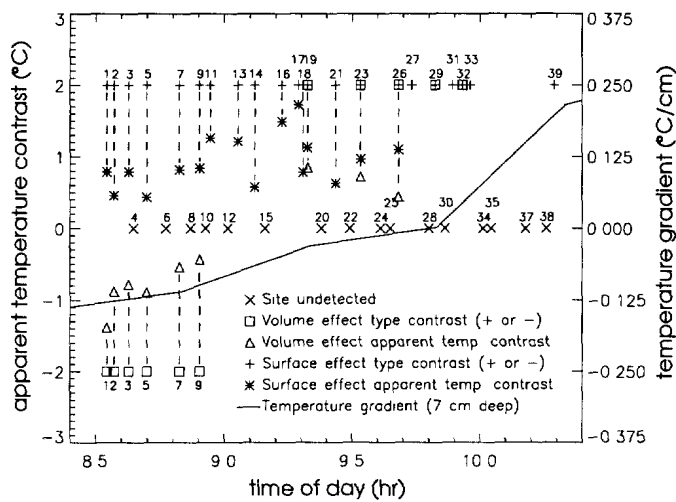
In addition to the data recorded during the different passes, information was also gathered on the spatial correlation of the temperature gradient along the road. To do so, a second temperature probe placed 3.5 km away from the first one but still on the same type of road (gravel packed road) was used. The temperature profile of this second probe was sampled manually once for each pass at a known time. The temperature contrasts derived from these temperature profiles were compared with those obtained with the first probe. The results are shown in figure 6.
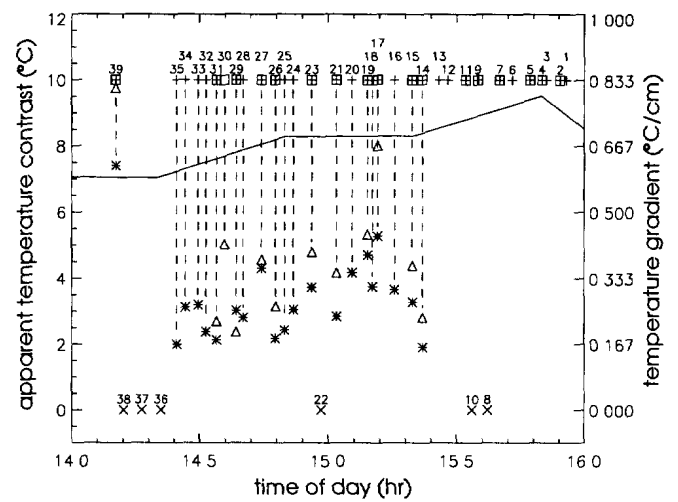
5   DISCUSSION

The results shown in figures 3 and 4 confirm a direct relationship between the temperature gradient and the temperature contrast as predicted above. This relationship can be approximated as linear where the linear coefficient linking the two temperature parameters decrease with the depth of the mine. Depending on the level of the heat flow into the ground and if the thermal volume effects of the mine are present exclusively, it has been observed that the IR signature cannot be observed if the mine is buried at a depth greater than 10 cm. However, hole effects [3], which allow the detection of mines buried at large depths, have been observed to last many months. During the different trials where the experimental data shown here was collected, it has also been observed that the volume effects give IR signatures specific to the types of mine buried. In addition to the volume effects, surface effects have been identified during sunny days. These effects are mainly present if mines are buried recently (few days) in compacted soils. It is these effects which cause the large standard deviation observed during day-time in the second static trial (see figure 4). The latter effects have the disadvantage of giving an imprecise position of the buried mines. At the present time, it is believed that these effects can be monitored using a radiation meter.

The results shown in figure 5 represent well the potential progress of a mine detection operation where the temperature gradient is used to predict the efficiency of the IR detector. The periods of the day associated with these four graphs have been chosen to cover the four main heat states of the road: the optimum periods during day and night (graph 5 b and 5 d), and the two transient periods (graph 5 a and 5 c). A first observation derived from these graphs is the weak correlation between the surface effect apparent contrasts (identified with star signs) and the temperature gradients (continuous lines) during the inversion periods. This supports the interpretation that the surface effect signature is not well described by the temperature gradient measured at a
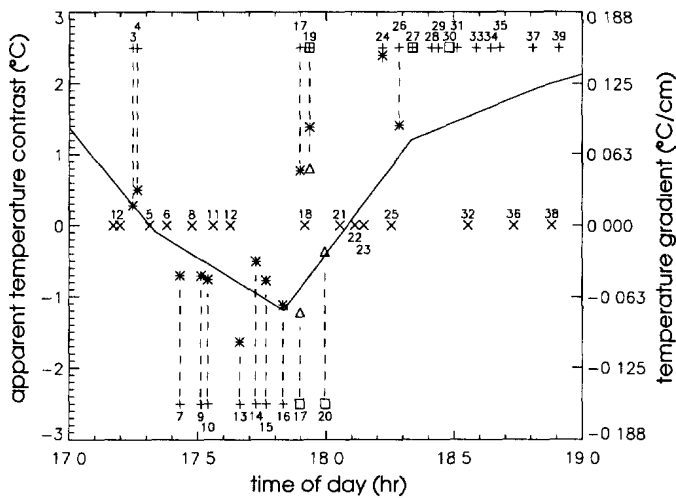
---

[3]The soil layer covering the mine does not have the same thermal conductivity as the surrounding soil.
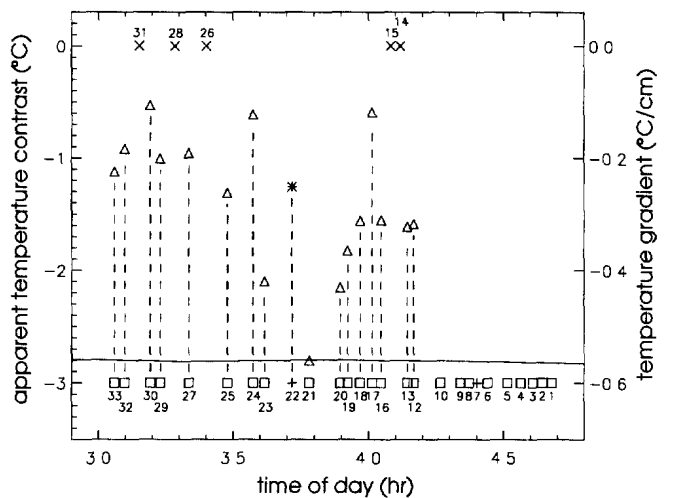
Figure 5: These four graphs show the apparent contrasts (created by surface and by volume thermal effects) and the temperature gradients as functions of time during dynamic trials. Graph a) was recorded during morning inversion period, graph b) was performed during the optimum day-time period, graph c) shows the effect created by a short light rain shower near the evening inversion period, and graph d) was taken during optimum night-time. Graph d) was obtained on a sand road. Graphs a), b), and c) were done on a packed gravel road.
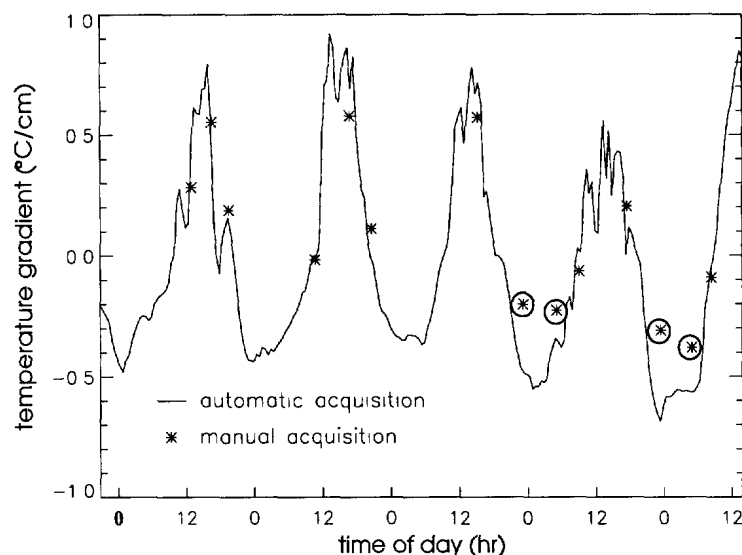
Figure 6: Graph showing the evolution of the temperature gradient over a week for two sites separated by 3.5 km. These two sites were on the same packed gravel road. The reading of one temperature probe was recorded automatically every half hour while the second one was sampled manually once after each dynamic trial. The circled data points represent four cases where the temperature gradient correspondence between the two sites were poor.

depth of 7 cm and could be intrinsically related to the atmospheric radiation level or the temperature gradient at the atmosphere-soil interface. Moreover, the results shown in graph 5 c where a 15-minute light rain shower occurred around 17:30 show the fast reaction time of the surface effect IR signature. This is in agreement with the low heat reactance associated with an effect localised close to the surface. On the other hand, we can observe that the IR signatures associated with the volume effect (identified by triangles) follow well the fluctuation of the temperature gradients especially during the inversion periods. During these trials, the mines were buried at depths varying from less than 1 cm to 5 cm. We can verify, for the passes done on packed gravel road (graphs 5 a, 5 b,and 5 c), that the ratio between the apparent temperature contrasts associated with the volume effect and the temperature gradients are comparable with the linear coefficients derived in figures 3 and 4. However, the same ratio derived with figure 5 d, a pass done on a sand road, is lower than that associated with gravel packed road. That could be explained by the lack of hole effects for mines buried on sand roads. Finally, it is interesting to observe that the detection efficiency [4] is maximum during the two optimum periods, as expected.

Another aspect investigated during the different trials reported here is the dependence of the correlation between the temperature contrast and the temperature gradient with the type of road and with the position where the temperature gradient is measured. First, from the results presented in the previous section, it seems that the linear coefficient linking these two parameters fluctuates little for mines buried at similar depth in packed gravel roads at different Canadian geological regions. This can be explained by the fact that soil thermal properties do not change much (thermal resistivity = 50-90 °C-cm/W over 100 sites in Canada[9]) when compared with common explosives such as TNT (thermal resistivity = 680 °C-cm/W[10]). Furthermore, as shown in figure 6, the spatial correlation of the temperature gradients seems acceptable even if a distance of 3.5 km separates the two measurement sites. It is anticipated that this correlation will remain acceptable as long as the measurement sites are under similar environmental conditions. However, it has been observed that severe weather conditions

---

[4]The detection efficiency on these graphs is described by a square symbol when the detection is associated with a volume effect and a plus symbol when the detection is associated with a surface effect. A value of +1 or -1 for these symbols indicates a positive or negative contrast. A time symbol designates an undetected site.

such as rain, snow or wind for the case of a sand road could seriously affect the heat dynamics between the soil and the atmosphere and make the correlation between the temperature contrast and the temperature gradient unusable.

Even with these limitations, it is believed that the correlation between the temperature contrast and the temperature gradient can be used in peacekeeping operations where mined road clearances are performed using IR technology. In such, a first step would be the measurement of the temperature contrast threshold for easy IR detection. For example, a threshold of -0.5 °C during night-time and +2 °C during day-time might be chosen from experimental testing. The higher contrast threshold for positive contrast is dictated by the higher clutter (thermal noise) present on road surfaces during day-time. With these temperature contrast thresholds defined, corresponding temperature gradient limits are identified using correlation graphs such as shown in figures 3 or 4 as a function of the expected depth of the buried mines. In an operational scenario, the temperature contrast could be sent automatically to the operator of the IR detector by radio link so that continuous update on the expected temperature contrast can be provided which could improve greatly the operator's trust in the technology.

6   CONCLUSIONS

In order to improve the usefulness of the IR technology in detecting buried mines for the Canadian National Defence Improved Land-Mine Detection Capability (ILDC), a new methodology has been evaluated. This methodology, derived from simple models, involves the measurement of the heat flow balance between the atmosphere and the soil layers by quantifying the ground temperature gradient. This approach has been tested during simulations of operational scenarios and a good linear relation between the temperature contrast of buried mines and the temperature gradient into the soil is reported.

7   ACKNOWLEDGEMENTS

8   REFERENCES

[1] C. Nelsen, Airborne minefield detection and reconnaissance system (AMIDARS), in *Proceedings of SPIE: Airborne Reconnaissance X*, pages 9–13, San Diego, CA, USA, 1986.

[2] A. Lareau, Photogramm Eng Remote Sens **57**, 173 (1991).

[3] S. Johnson, Minefield reconnaissance and detector (MIRADOR) utility study, Final Technical Report Cont. DAAK70-88-D-0015, Wackenhut Advanced Technology Corp., 1989.

[4] E. C. B.H. Miles and A. Goodson, Polarization-based active/passive scanning system for minefield detection, in *Proceedings of SPIE No.1747: Polarization and Remote Sensing*, pages 239–252, San Diego, CA, USA, 1992.

[5] P. M. J.N. Muczynski, R.J. Horner and J. Salinger, Remote minefield detection system (REMIDS) real-time processing architecture study, Technical Report ERIM-208600-1-T, Environmental Research Inst. of Michigan (ERIM), 1988.

[6] N. D. Grande, Sensor fusion methodology for remote detection of buried land mines, in *Proceedings of the 3rd National Symposium on Sensor Fusion*, Orlando, Florida, USA, 1990.

[7] N. D. Grande et al., Dual-band infrared capabilities for imaging buried object sites, in *Proceedings of SPIE No.1942: Underground and Obscured Object Imaging and Detection*, pages 166–177, Orlando, Florida, USA, 1993.

[8] M. Firdaouss, C. R. Acad. Sc. Paris **297**, 105 (1983).

[9] J. E. Steinmanis, Thermal properties database of canadian soils, Technical report, Geotherm Inc., 1989.

[10] D. L. Patel, Handbook of land mines and military explosives for countermine exploitation, Technical Report (Defence Purposes Only) USA-BRDEC-TR // 2495, United States Army, 1992.

514412